Available online at www.sciencedirect.com
SCIENCE DIRECT
Remote Sensing of Environment 102 (2006) 223–236
Remote Sensing of Environment
www.elsevier.com/locate/rse

Automated assessment of hardwood and shrub competition in regenerating forests using leaf-off airborne imagery

D.A. Pouliot [a], D.J. King [a,*], D.G. Pitt [b]

[a] Department of Geography and Environmental Studies, Carleton University, 1125 Colonel By Drive, Ottawa, Ontario, Canada K1S 5B6
[b] Canadian Forest Service, Great Lakes Forestry Centre, P.O. Box 490, Sault Ste. Marie, Ontario, Canada P6A 5M7

Received 20 June 2005; received in revised form 3 February 2006; accepted 9 February 2006

Abstract

Forest regeneration assessment considers the abundance and condition of crop trees as well as the level of competing vegetation. Most remote sensing research has been conducted on conifer crop tree detection and assessment using imagery acquired in deciduous leaf-off conditions. Some research on competition assessment has been conducted using leaf-on imagery, but it is too costly and time consuming to require both leaf-off and leaf-on image acquisition and analysis for complete regeneration assessment. This paper evaluates the potential of automated methods for assessment of woody stem competition using very high-resolution (2 cm) leaf-off imagery. The intent is to couple the competition-evaluation methods with previously developed leaf-off conifer assessment methods. The automated method combined texture analysis, classification, and line detection. Results show that competition measures extracted from the processed imagery agreed well with estimates derived from both manual competition interpretation and field measurements. Manual estimates slightly outperformed automated extraction when compared against field measurements, but the best approach may be to combine them to optimize processing time and achieve the highest possible precision, particularly in areas where competition abundance is estimated to be close to a given silvicultural decision threshold.

Keywords: Competing vegetation; Classification; Texture; Line detection; Modelling

1. Introduction

Sustainable forestry depends on successful forest re-establishment after disturbance. In the boreal region, regeneration of coniferous species can be difficult due to the effects of competing vegetation, which reduces light, moisture, and nutrients to desired crop trees. It is widely recognized that for timely and effective coniferous forest re-establishment some form of competition control is required (Wagner et al., 2001; Walstad & Kuch, 1987; Wang et al., 2000). Typical control options include chemical sprays and a few types of manual extraction or cutting of competition. Determining the optimal level and timing of control is a complex and largely subjective process designed to balance the objectives of crop tree success and cost of re-establishment with other ecological considerations such as soil stability and productivity, nutrient availability, temperature regulation, and wildlife habitat concerns. Further, retention of some competing vegetation can be used to control crop tree form for various end use applications such as dimensional or pulp products (pers. comm. Bell, 2001).

The influence of competing vegetation on the establishment and growth of desired crop trees has prompted research in the field of vegetation management in order to quantify and more clearly understand the relations between competitor and crop growth. One facet of this discipline is the parameterization of competition and crop attributes to aid in identification of practical methods for evaluating competition effects on crop trees and to provide input to competition control decision making in operational forest management. To date, considerable research has been undertaken to develop field based measurements that relate crop growth to measurable competitor attributes such as visually estimated cover, height, proximity,

* Corresponding author. Tel.: +1 613 520 2600x8439; fax: +1 613 520 4301.
E-mail addresses: darren.pouliot@CCRS.NRCan.gc.ca (D.A. Pouliot), doug_king@carleton.ca (D.J. King), dpitt@NRCan.gc.ca (D.G. Pitt).

0034-4257/$ - see front matter © 2006 Elsevier Inc. All rights reserved.
doi:10.1016/j.rse.2006.02.008

and light interception (Bell et al., 2000; Burton, 1993; Comeau et al., 1993; Morris et al., 1990; Ter-Mikaelian et al., 1999).

Remote sensing research in regeneration assessment has been primarily concerned with assessment of the abundance, spatial distribution, and condition of conifer crop trees using leaf-off imagery (Brown & Fletcher, 1999; Goba et al., 1982; Gougeon & Leckie, 1999; Hall, 1984; Hall & Aldred, 1992; Pouliot & King, 2005; Pouliot et al., 2002, 2005; Price & Davison, 1999). It has not been widely researched for competition assessment. Of the few previous studies, leaf-on aerial photography has been used for identification of general cover types (e.g., Pitt & Glover, 1993; Pitt et al., 2000) and high resolution (2.5 cm) digital camera imagery has been assessed for cover and leaf-area estimation (Haddow et al., 2000). Leaf-on conditions provide the best opportunity to assess competition because leaves are clearly visible to the sensor. However, it is difficult, if not impossible, to assess coniferous crop tree attributes in these conditions because the trees are either hidden from the sensor or cannot be easily distinguished from the surrounding competing vegetation. Conversely, leaf-off conditions provide a clear view of coniferous crop trees, but competition is not easily evaluated. This requirement for two sampling periods to satisfy overall objectives of both conifer and competition evaluation has hindered the adoption of remote sensing in operational regeneration assessment.

The purpose of this research was to evaluate the potential of high-resolution leaf-off imagery to assess deciduous woody competition abundance. If successful, the methods could be coupled with conifer assessment methods that also use leaf-off imagery (e.g., Pouliot et al., 2002, 2005). Automated data extraction from imagery was evaluated for modeling field based measures of competition abundance and compared to estimates derived from manual interpretation as well as field measurements. As this is the first known study of competition assessment using leaf-off imagery, some background on the characteristics of woody competition in high-resolution leaf-off imagery is provided to justify the methodological approach that was taken. The approach integrated common automated methods of classification, texture analysis, and morphological feature extraction to establish a base from which longer term research could be developed.

2. Methods

2.1. Study sites

The study sites consisted of three operational cutovers northeast of Sioux Lookout, Ontario in the Buchanan Inc. forest management unit. The three cutovers represented various regeneration conditions typical of the region that reflected soil and microclimate conditions. They were labeled High (50°46′ N, 91°25′W), Moderate (50°18′N, 91°39′W), and Low (50°50′ N, 91°21′W) based on competition intensity. Conditions at these sites were presented in detail in Pouliot et al. (2005) so, for brevity, only the information relevant to competing vegetation is presented here. Fig. 1 shows example ground conditions and competition levels at each site.

The High site supported a variety of herbaceous and woody competition species indicative of rich soil with moderate moisture. Woody vegetation was abundant with a mean density of 8500 stems per hectare (sph) for trees above 2 m in height. This layer was dominated by alder (*Alnus* spp.), but also contained aspen (*Populus tremuloides*), white birch (*Betula papyrifera*), willow (*Salix* spp.), red-osier dogwood (*Cornus stolonifera*), and beaked hazel (*Corylus cornuta*). Grass was the most abundant herbaceous vegetation, occurring in patches where woody competition density was low.

Competition at the Moderate site consisted of pockets of high-density aspen and lower density birch with a mean density of 3400 sph for trees above 2 m in height. Aspen tended to be considerably taller than birch. Herbaceous vegetation was dominated by grass and moss in moist depressions. In higher areas, various low woody shrub types were abundant.

The Low site had little to no competing woody vegetation greater than 2 m in height. Woody species included alder and willow, while herbaceous competitors included Labrador tea (*Ledum groenlandicum*), mosses, lichens, and some sparse grasses.

2.2. Field data

Circular sample plots of 3 m radius were subjectively selected along a pre-determined transect in order to represent the full range of conifer tree species, tree density, crown sizes, and woody competitor abundance at each site. For visual

Fig. 1. Example ground conditions at each site. Left — High transect, middle — Moderate transect, right — Low transect.

reference in the airborne imagery, plot centers were marked with a 40×40 cm white board, mounted on a 1.0 m tall stake. The height of each woody stem in the plot that was taller than 0.5 m was recorded.

Two field measures of competition abundance were evaluated as dependent variables: stem density and a simple competition index (CI) for three height classes, >0.5, >1, and >2 m. CI was calculated as the sum of woody competition heights in the plot above the defined height threshold. Stem density is a more intuitive measure of competition abundance and is typically used as the minimum information requirement for competition control treatment decisions. However, CI captures both height and density information.

2.3. Image data

Initially, two sensor types were assessed for this study: multispectral CIR digital camera imagery with 6 cm pixels (as used for conifer assessment in Pouliot et al., 2005) and 1:760 scale 70 mm colour photography scanned to 2 cm pixels. The digital camera image pixel size was not quite small enough to discern woody competition stems so the photography was selected. It was acquired on May 11, 2002 between 11:30 and 15:00 using a Hasselblad aerial camera with a 100 mm focal length lens. The camera was mounted in a boom system attached to the undercarriage of a Bell Ranger helicopter and flown at 185 m above ground. The 5-in. prints were scanned at 1000 dpi pixel density using a standard desktop scanner. Plots were extracted as 600×600 pixel subsets and concatenated into a single image file for processing. In total, 79 plots were extracted; 43 from the High, 21 from the Mod, and 16 from the Low transects. Different numbers of plots were used due to constraints on the imagery for the analysis requiring imagery only from the backscatter direction (see next section). The High site data contained most of the variance in competition levels, the Moderate site most of the remainder, while the Low site did not contain any detectable competition. The Low site was included to increase the variance of other scene components such as soil, slash, and rock, which are often present in operational conditions and which can have similar spectral and spatial image characteristics to woody competition.

2.4. Distinctive image properties linked to competition abundance

Examination of the imagery revealed several potentially useful image properties of competing shrub and hardwood vegetation (Fig. 2). Spectral properties of branches, stems, and reproductive structures were often distinct, but in some places they were similar to other cover types. For example, hardwood competitors such as poplar and older birch generally had grey–white stems and branches that appeared spectrally similar to rock and snow, which were present in localized patches. Fortunately, their spatial structures were quite different with their straight stems being more visible with increasing view angle in the backscattering direction (i.e. relative azimuth between sun and sensor <180° (Lillesand & Kiefer, 2000), as in Fig. 2A). Potential was evident for both image texture and linear feature (stem) extraction and analysis. In the forward scattering region of the image (i.e. relative azimuth between sun and sensor >180°), hardwood stems were not clearly visible. Hardwood shadow presence, size and form (Fig. 2B) were also initially considered as possible characteristics for assessment of competition type and abundance. Shadows were more distinctive in the forward scattering direction if the background was relatively uniform. However, shadows cast on dark ground were difficult to detect and shadows cast by proximal objects such as a conifer crown and a hardwood stem can overlap (as shown in Fig. 2C). These were common occurrences in the imagery so shadow analysis was not considered further.

Shrub competition such as alder, willow, and hazel generally had brownish woody structures (Fig. 2D) that appeared spectrally similar to soil cover (Fig. 2E), especially for wetter soils. Shrubs did not have specific structural properties associated with sun-sensor geometry as did hardwoods, but they did appear to have some potentially useful texture properties that were distinctive from soil.

Based on these visually distinctive hardwood and shrub properties, spectral, textural and morphological analyses were conducted and integrated into the competition assessment methodology described below.

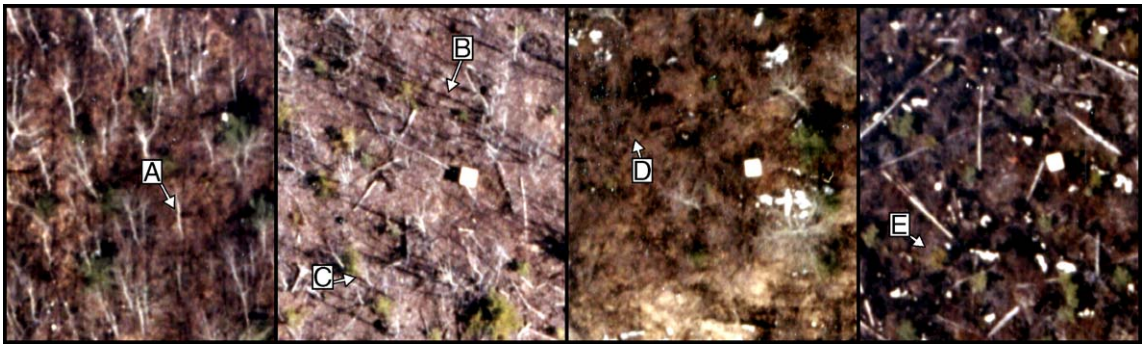

Fig. 2. Characteristics of competition in leaf-off imagery. A) hardwood stems in the backscatter portion of the image, B) clearly visible hardwood stem shadows, C) obstructed hardwood stem shadow, D) shrub competition, E) soil that can appear spectrally similar to shrub competition.

2.5. Extraction of hardwood and shrub competition abundance measures

Measures of competition were extracted from the imagery manually using visual interpretation and with an automated algorithm. These measures were then used to develop models with the field measurements of stem density and CI.

The imagery used for hardwood stem extraction was restricted to view angles greater than 4° in the backscatter direction as stems of poplar were most distinct in this region. The manual and automated analyses were designed to estimate the number of stems, average stem length, and total number of stem pixels within the image plots. Stem length was standardized to remove distortions due to relief displacement (Eq. (1)) within the given image view angles (4° to 17°).

$$h = \frac{dH}{r} \tag{1}$$

where h is the true object height, H is the flying height, d is the measured displacement of the object in the image, and r is the distance from nadir to the top of the image object (Lillesand & Kiefer, 2000).

View and scattering angle images, following the methodology given in Pellikka et al. (2000), were produced for each image and the mean values for both were extracted for each plot. This information was used to evaluate whether these variables were significant in multiple regression competition models by accounting for sun-sensor geometry effects.

For shrub competition, total cover (number of pixels with shrub presence) was extracted as well as a fuzzy measure of total cover. The purpose of the fuzzy measure was to make the cover estimates more robust by providing a graded estimate of cover instead of a hard classification of shrub/no-shrub for each pixel. The fuzzy cover (FC) estimate was based on Euclidean distance calculated as:

$$\mathrm{FC} = \frac{1}{1 \times 10^5} \sum_{i=1}^{n} \left[442 - \sqrt{\sum_{j=1}^{m} (x_{ij} - \bar{x}_j)^2} \right] \tag{2}$$

where i is a shrub cover pixel, n is the number of shrub pixels in the plot, x_{ij} is the pixel value for band j, $\bar{x}_j$ is the mean value for the band j computed from the training sample pixels, and m is the number of bands. The constant 442 represents the maximum Euclidean distance value attainable with 3-band 8-bit data and is used to reverse the scale of the data such that pixel values closer to the mean represent larger values than those further away. Thus, as FC increases shrub competition also increases.

2.5.1. Manual interpretation of competition properties

Manual interpretation was undertaken as part of an initial exploratory analysis to identify potentially useful image features unique to shrub and hardwood competition as described above. It was not the focus of this study, but the results were found to be useful in comparison against the automated processing results. It was accomplished by first training the interpreter (first author) on a subset of image data containing ground truth to recognize the properties of hardwood and shrub competition. Field measurements and pictures taken of the plots from different perspectives on the ground were used to aid training. Twelve plots were used for training, 5 plots from the High transect, 4 from the Moderate transect, and 3 from the Low transect. For hardwood competition, a line representing the stem was manually digitized. For shrub competition, identified areas were digitized as polygons. Both were conducted independently of the automated algorithm processing described below.

2.5.2. Automated extraction of competition image properties

Automated image analysis methods were explicitly selected to capitalize on the spectral, spatial and structural image properties of competing vegetation as discussed above.

2.5.2.1. Classification and texture analysis. Supervised maximum likelihood classification was applied using nine classes: shrub, hardwood, shadow, snow-rock, conifer, grass, light soil, dark soil, and red colored soil. For each class, six plots were selected and three samples were taken within each plot. Plots and the samples they contained were then assigned randomly as either training or validation data. Thus, for each class nine samples were used for training and nine for validation. Separate classifications were conducted for hardwood and shrub to optimize the spectral and textural features used for each of these classes.

Co-occurrence texture measures were used, as they are commonly applied for extraction of forest information at a variety of scales (Franklin et al., 2000; Haddow et al., 2000; Peddle & Franklin, 1991; Treitz & Howarth, 2000; Tuominen & Pekkarinen, 2005; Wulder et al., 1996) and have the potential to discriminate between a large number of determinate and statistical patterns. They are based on the co-occurrence matrix, which tabulates the probability of pairs of pixel gray-levels within a sample window. Several measures of texture can be derived from the matrix (e.g., Haralick et al., 1973). For a given texture measure there are several parameters that must be considered: 1) sample window size, 2) inter-pixel sample distance, 3) inter-pixel sample direction, and 4) quantization level. Selection of the most discriminating texture measure and the best parameter set for a given texture measure is not straightforward and typically involves trial and error or an automated computer intensive approach. As this was the first study of its type, the computer intensive approach was used. Texture measures included Homogeneity (HOM), Contrast (CON), Mean (MN), Variance (VAR), Entropy (ENT), Dissimilarity (DIS), and Angular Second Moment (ASM). Window size was varied from 5 to 47 pixels in a 7-pixel step interval. The upper limit was selected as the largest size that could be used with minimal class boundary crossings. The spatial variability of each class was high with many small patches on the order of one to a few meters in size. Thus, we felt that a window size of 47 pixels (94 × 94 cm) was the largest that should be considered. It also represented a reasonable upper limit for processing time, which increased exponentially with window size (~20 h for the 47 × 47 window and the

7300×4300 image database). Inter-pixel sample distances of 1, 3, and 5 pixels were tested. Directionally invariant sampling of pixel pairs was used because no distinct directional properties were visible in the imagery. Quantization was held constant at 6 bits (64 gray levels). These texture measures are subsequently referred to by their 'acronym_window size_pixel spacing' as in the following example: HOM_5_1 (Homogeneity with 5×5 window size and sample distance of 1 pixel). CON and VAR were non-normally distributed so a log transformation was applied.

The output image for each texture measure was included with the three original spectral bands to calculate the Jeffries–Matsushita (J–M) separability measure (Richards, 1993) for the hardwood and shrub classes as shown in Eq. (3).

$$JM_{ij} = 2 \times (1 - e^{-a_{ij}}) \tag{3}$$

where

$$a_{ij} = 0.125 \times (M_i - M_j)^T \times (C_a)^{-1} \times (M_i - M_j) + 0.5 \times \ln(|C_a| \div (|C_i| \times |C_j|)^{0.5}) \tag{4}$$

M_i, M_j = mean vectors for class i or j;
C_i, C_j = Covariance matrix for class i or j;
C_a = $(C_i + C_j)/2$.

The minimum separability between the hardwood or shrub class and one of the other classes was used to compare the classification potential of the different texture measures. A simple leave-out resampling approach was used to reduce the dependence of the separability measure on training data. For each iteration, seven of the nine samples for each class were randomly selected and used to calculate separability. The mean and lower 95% bound of the J–M distance for 30 iterations were calculated and used to compare the texture measures.

Because of the high correlation between some co-occurrence texture measures (Hall-Beyer, 2004), they were grouped to minimize between group correlations. The best measure from each group was used in classification in order maximize the amount of independent information in the input variables. Three groups were identified based on Hall-Beyer (2004): 1. *Contrast* — HOM, CON, VAR, DIS; 2. *Orderliness* — ENT, ASM; 3. *Descriptive* — MN.

Finally, as very high-resolution imagery can be strongly influenced by local noise, a Gaussian noise reduction filter (GF) with standard deviation (σ)=1 was evaluated for potential classification improvement.

To evaluate hardwood or shrub class accuracy in each of the classifications, the conditional kappa coefficient was used.

$$\mathrm{KU}_i = \frac{N(x_{ii}) - (x_{i+} \times x_{+i})}{N(x_{i+}) - (x_{i+} \times x_{+i})} \tag{5}$$

where KU_i is the user's kappa coefficient for class i, N is the total number of sample pixels, x_{ii} is the number of correctly classified pixels, x_{i+} equals x_{ii} plus commission error, and x_{+i} equals x_{ii} plus omission error. For producer's accuracy (KP_i) the denominator in Eq. (5) becomes $N(x_{+i}) - (x_{i+} \times x_{+i})$. To obtain a measure of class accuracy that accounts for both omission and commission error, the average of KU_i and KP_i was taken (KA_i).

2.5.2.2. Line detection. Line detection of hardwood stems was accomplished using a slightly modified version of Steger's (1998) method. This involved determination of the optimal scale, identification of candidate line points, and linking points into lines. Modifications to Steger's criteria included how candidate line points were selected and linked to create lines.

Optimal detection for a given line width is dependent on image scale. For line detection, the relation between the minimum smoothing level and line width is $\sigma \geq w/\sqrt{3}$, where w is the line width and σ is the standard deviation parameter used in Gaussian filtering (Steger, 1998). In this study, hardwood stems were generally about 3 pixels wide. Thus, $\sigma = 2$ was selected for Gaussian smoothing before implementation of the line detection algorithm.

The radiometric topography of linear features in an image consists of narrow valleys if they are dark or ridges if they are bright. In one dimension, the location of a ridge is where grey-level values perpendicular to the line have a first derivative value of zero and local minima in the second derivative. To detect lines in two-dimensions the derivatives in the horizontal, vertical, and diagonal directions can be found for the image $f(x, y)$ using convolution masks. The masks are: $f_x = [-1\ 1] * f(x,y)$ (horizontal), $f_y = [-1\ 1]^T * f(x,y)$, (vertical), and $f_{xy} = [-1\ 1]^T * f_x$ (diagonal), where T indicates the transpose. The second derivatives in the x and y directions, f_{xx} and f_{yy}, are obtained by convolving the first derivative responses with these same masks. These values define the Hessian matrix as:

$$H(x,y) = \begin{bmatrix} f_{xx} & f_{xy} \\ f_{xy} & f_{yy} \end{bmatrix} \tag{4}$$

where the maximum absolute eigenvalue of the Hessian matrix gives the line strength and the associated eigenvector gives the perpendicular direction to the line as a unit vector (n_x, n_y). The sub-pixel position of the line can then be calculated as:

$$t = \frac{f_x n_x + f_y n_y}{f_{xx} n_x^2 + 2 f_{xy} n_x n_y + f y_y n_y^2}. \tag{5}$$

A point is considered a line if $(tn_x, tn_y) \in [-1/2, 1/2] \times [-1/2, 1/2]$. In this implementation, a further constraint for acceptance of line points was applied to ensure that the line direction had an orientation similar to that of the imaginary line joining the pixel and nadir (the pixel azimuth), as stems should appear to be leaning away from nadir in this direction due to view angle/relief displacement. A tolerance of 10° was used for this criterion based on visual assessment of several threshold tests.

As in Steger (1998), to link detected line points, local maxima positions were identified with a 3×3 local maximum filter and used as starting points for line following. For each, line following was performed by moving to the next pixel in a

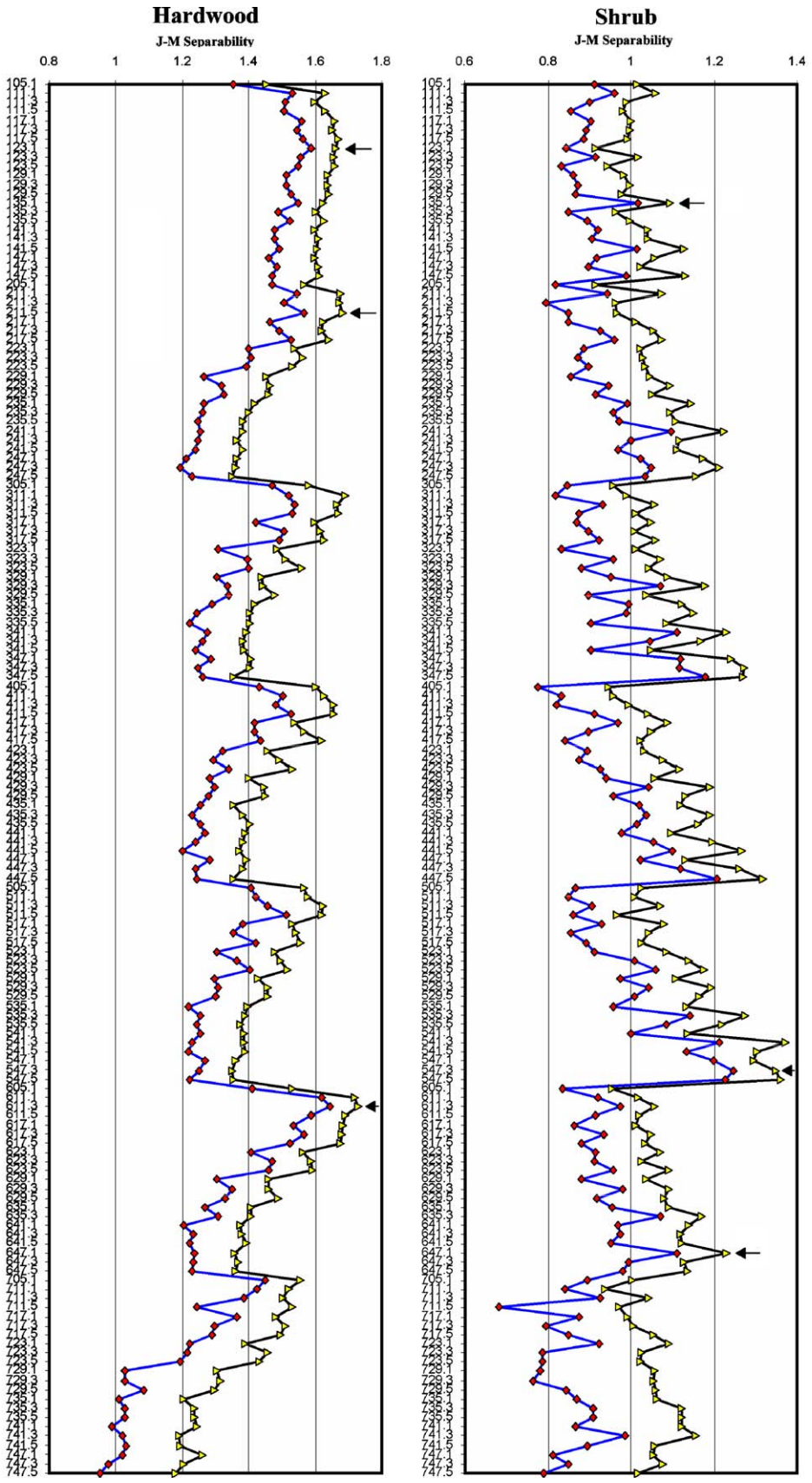

Fig. 3. Hardwood and shrub class separability results for the original RGB bands with an additional texture measure. Values are the mean (triangles) and lower 95% confidence bound (−2 s, diamonds) obtained from 30 iterations of resampled training data. For display purposes the graphs have been rotated, the *x*-axis is the J–M separability measure and the *y*-axis is the texture measure label. The first digit in the label identifies the method (1—MN, 2—VAR, 3—HOM, 4—CON, 5—DIS, 6—ENT, 7—ASM). The following two digits give the window size and the decimal number is pixel sample distance. Arrows identify the texture measure that produced the highest minimum separability for each of the defined texture measure groups.

3×3 window that maximized the line strength (l_s) and minimized the angular difference between lines (l_a). Line strength and angular difference were scaled to 0–1 by dividing by their maximum respective values in the image. For angular difference, the scale was reversed by subtracting the maximum angular difference such that larger angular differences took on small values of l_a and small differences took on large values. Line strength and angular difference were summed as $l_s+0.5l_a$. In this implementation, line strength was considered to be more important for line following than the distance between candidate line points as used in Steger's implementation because thresholding on line strength was not used. Instead, the final lines were extracted as the intersection of line points with the hardwood classification results. Further, small lines less than 5 pixels long were removed.

2.6. Modeling hardwood and shrub competition abundance

Correlation analysis and stepwise least squares regression were used in initial exploratory analysis to determine meaningful variables for competition modeling. However, the use of least squares regression can lead to biased estimates of regression parameters if errors in the independent variable are large compared to that of the dependent variable (Draper & Smith, 1998). To account for this in final model parameter estimates, geometric mean regression was used, which is a robust estimator in this situation (Draper & Smith, 1998). For hardwoods, models were explored for the following variables: average stem length/plot, number of stems/plot, total stem length/plot, mean plot view angle, and mean plot scattering angle. In addition, average stem length/plot and total stem length/plot (STSL) were standardized by view angle and evaluated. For shrubs, total shrub pixel count/plot, a fuzzy pixel count/plot (FZCN), mean plot view angle and mean plot scattering angle were evaluated.

It was also desirable to develop a model that could be used to predict the level of both shrub and hardwood competition combined (hardwood+shrub). This was accomplished by combining the individual shrub and hardwood models and simplifying (i.e. if shrub$=m_s$FZCN$+b_s$ and hardwood$=m_h$STSL$+b_h$, then hardwood+shrub$=m_s$FZCN$+b_s+m_h$STSL$+b_h$). It is appropriate in this case because these variables were only correlated with their associated dependent variable. All other combinations of correlations between dependent and independent variables for these two models were low ($r<0.2$).

To evaluate model robustness and predictive ability, an iterative resampling procedure was applied. Resampling analysis with a 1/3 data leave out rule was used with 1000 iterations. The means and standard deviations were obtained for the model parameters (a and b), modeling efficiency statistic ($EF = 1-\sum(y_i-\hat{y})^2/\sum(y_i-\bar{y}_i)^2$ for the line $y=\hat{y}$ Mayer & Bulter, 1993), model bias ($BIAS = [\sum y_i-\hat{y}_i]/n$), and mean absolute error ($MAE = [\sum |y_i-\hat{y}_i|]/n$). The average of each of these goodness of fit statistics is reported for the 1/3 validation sample from the 1000 iterations.

3. Results

3.1. Extraction of hardwood and shrub abundance measures

3.1.1. Evaluation of texture for competition classification

The results of the texture analysis showed that the minimum separabilities of both the hardwood and shrub competition classes were low (Fig. 3). For hardwoods, the minimum separability was with the snow/rock class. Window size had the most substantial effect followed by the type of texture measure. Increasing the sample window size decreased the separability. Most of the texture measures produced similar results, however, the MN measure was least affected by window size and ASM produced considerably

Table 1
Classification accuracy for the selected feature combinations used in classification

	Data features	Total samples	Correct	Commission error	Omission error	User's kappa KU_i	Producer's kappa KP_i	Average kappa KA_i
Shrub	RGB	33,637	9407	726	2465	0.889	0.703	0.796
	RGB_GF	33,637	10,464	245	1408	0.965	0.826	0.895
	RGB+S1	33,637	8756	609	3116	0.899	0.636	0.768
	RGB+S2	33,637	9084	642	2788	0.898	0.670	0.784
	RGB+S3	33,637	9777	350	2095	0.947	0.748	0.847
	RGB_GF+S1	33,637	9541	237	2331	0.963	0.723	0.843
	RGB_GF+S1,S2	**33,637**	**10,603**	**185**	**1269**	**0.973**	**0.843**	**0.908**
	RGB_GF+S1,S2,S3	33,637	10,394	177	1478	0.974	0.818	0.896
Hardwood	RGB	33,637	866	806	62	0.504	0.930	0.717
	RGB_GF	33,637	887	765	41	0.524	0.954	0.739
	RGB+H1	33,637	888	1025	40	0.449	0.954	0.702
	RGB+H2	33,637	847	1161	81	0.405	0.907	0.656
	RGB+H3	33,637	895	987	33	0.461	0.962	0.712
	RGB_GF+H1	33,637	900	881	28	0.491	0.968	0.730
	RGB_GF+H1,H2	33,637	898	1127	30	0.428	0.966	0.697
	RGB_GF+H1,H2,H3	**33,637**	**896**	**303**	**32**	**0.740**	**0.964**	**0.852**

Commission and omission errors in training and test columns are in numbers of pixels.
GF — Gaussian filtered, S1 — DIS_47_3, S2 — ENT_41_1, H1 — ENT_11_3, H2 — MN_23_1, H3 — VAR_11_5.

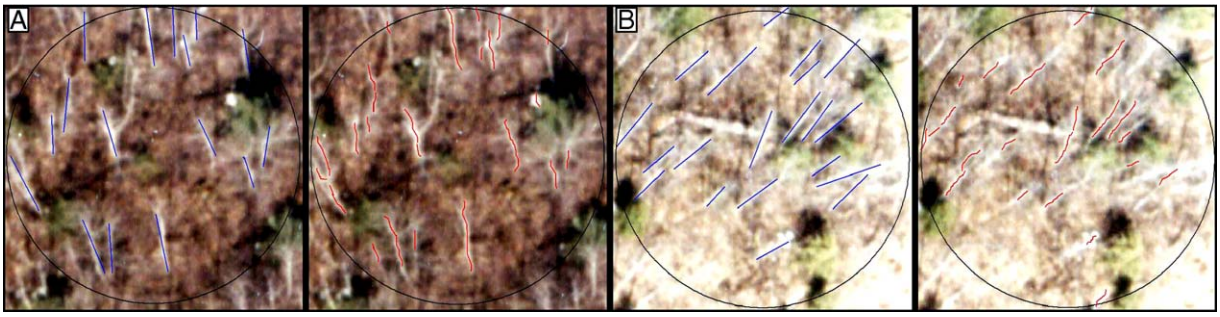

Fig. 4. Example results of hardwood stem detection. In each example the visually interpreted results are on the left and colored blue while the automated results are on the right and colored red.

lower separabilities. ASM actually decreased the separability compared to that for the original RGB bands alone. No trend was apparent for sample distance. The best texture measures for each of the defined groups for hardwood discrimination were: 1. *Contrast* — VAR_11_5; 2. *Orderliness* — ENT_11_3; and 3. *Descriptive* — MN_23_1. These texture measures are indicated by the arrows in Fig. 3.

For shrubs, separabilities with other classes were lower than for hardwoods due to a strong spectral similarity with the dark soil class. Window size had the most influence on separability, but in this case, increasing it resulted in increased separability. As with the hardwood results, ASM produced the lowest separability, but it was greater than that of the original RGB bands alone (J–M = 0.84). No trend for sample distance was identified. The best texture measures for each of the defined groups were: 1. *Contrast* — DIS_47_3; 2. *Orderliness* — ENT_47_1; and 3. *Descriptive* — MN_35_1.

Both the hardwood and shrub separability results show that for some texture measures and input parameters, the difference between the mean and lower bound J–M distance varied amongst re-sampled training data iterations, indicating a dependence on the training data used. For example, ASM shows the largest difference for both the shrub and hardwood classes and thus appears to have been most affected by the training data used.

3.1.2. Classification results

Table 1 shows the classification accuracies for hardwoods and shrubs with different combinations of spectral and textural features. The hardwood class produced a moderate separability, but had low average kappa (KA) for almost all feature combinations tested. The shrub class was the opposite, with low separability and higher KA values compared to the hardwood class. This discrepancy resulted from the information utilized in the separability and KA measures, as separability only considered confusion between two classes at a time, whereas KA is a summary measure of confusion for the given class with all other classes. Gaussian smoothing and texture incorporation produced the best results for each class. For hardwoods, the optimal set of input features included all Gaussian filtered spectral bands and all the selected texture measures. A similar feature combination was found to be optimal for the shrub class, except that only the two best texture measures were included. These optimal feature combinations are bolded in Table 1.

3.2. Modeling hardwood and shrub competition abundance

In bivariate modeling of hardwood competition, STSL proved to be the best predictor using either manual or automated extraction. For shrub competition, total pixel count and FZCN were found to provide similar predictive ability. However, FZCN provided a slight improvement and is theoretically more resilient to classification errors than the hard pixel count, so it

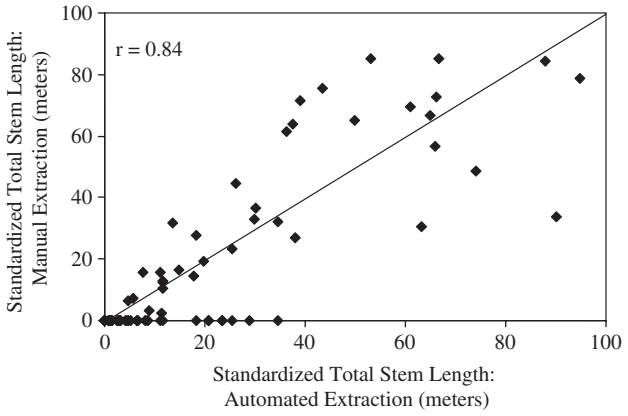

Fig. 5. Scatterplot of manual and automated standardized total stem length of hardwood stems per plot. The line depicts the relation $y=\hat{y}$.

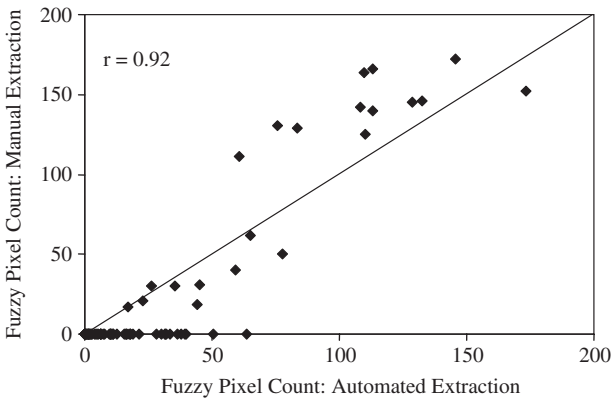

Fig. 6. Scatterplot of manual and automated fuzzy pixel counts per plot for the shrub class. The line depicts the relation $y=\hat{y}$.

was retained for further modeling. The mean plot view angle and scattering variables were not found to be significant in any of the multiple regression models evaluated. This suggests, that sun-sensor geometry effects were not as significant as other sources of dependent variable variance or that these effects were more complex than could be captured by a simple weighted sum of variable combinations.

3.2.1. Comparison of competition measures extracted using manual and automated methods

For hardwood competition, Fig. 4 is an example of the results of manual and automated line (stem) extraction for two plots. Overall, most of the same features were identified except several additional small lines were found by the automated algorithm and some lines were not fully connected.

Fig. 5 shows a scatterplot of STSL extracted using the manual and automated methods. The two measures were strongly correlated with observations equally distributed on either side of the idealized $y=\hat{y}$ line. Woody debris and other small linear features oriented in the same direction as that expected for hardwood stems were the main factors causing overestimation of STSL by the automated method. In some plots where there were no competing stems, the automated method made several commission errors leading to a large range in x for $y=0$, while the manual method was not subject to this error. At the high end of the data range (approximately 60–100 m), both the manual and automated methods were substantially more variable.

For shrub competition, Fig. 6 shows a scatterplot of FZCN extracted using manual interpretation and the automated procedures for each plot. The two measurements are strongly correlated, but the automated estimates are greater at the lower end of the data range and the manual results tend to be larger for larger values. As seen for hardwoods, there are many plots for

Table 2
Model results for the competition index (CI) measured in meters

Dependent variable	Mean	Stdv	Max	Independent variable(s)	Model parameters		Model fit statistics		
					Slope	Offset	EF	BIAS	MAE
CI_H_0.5	45	59	229	STSL_MAN	2.270	3.721	0.793	0.022	18.002
					0.161	*1.994*	*0.071*	*5.908*	2.345
CI_H_1	45	59	222	STSL_MAN	2.239	3.384	0.801	0.026	17.533
					0.155	*1.853*	*0.078*	*5.890*	*2.358*
CI_H_2	38	55	190	STSL_MAN	2.039	0.859	0.862	0.002	12.600
					0.135	*1.341*	*0.043*	*4.486*	*1.824*
CI_H_0.5	46	60	229	STSL_AUT	2.326	−3.226	0.660	0.590	21.350
					0.234	*2.251*	*0.133*	*7.775*	*3.038*
CI_H_1	45	59	222	STSL_AUT	2.283	−3.472	0.670	0.247	21.050
					0.228	*2.141*	*0.140*	*7.557*	*2.911*
CI_H_2	39	56	190	STSL_AUT	2.079	−5.343	0.677	0.138	19.218
					0.214	*1.847*	*0.130*	*7.069*	*2.724*
CI_S_0.5	45	64	262	FZCN_MAN	1.359	10.872	0.720	0.373	20.802
					0.129	*2.541*	*0.140*	*8.067*	*3.618*
CI_S_1	33	62	247	FZCN_MAN	1.176	1.713	0.836	0.050	13.415
					0.118	*1.466*	*0.083*	*5.590*	*2.539*
CI_S_2	22	52	220	FZCN_MAN	0.950	−2.966	0.787	−0.461	12.152
					0.132	*1.367*	*0.105*	*5.214*	*2.100*
CI_S_0.5	47	65	262	FZCN_AUT	0.152	−3.424	0.586	−0.208	27.046
					0.019	*3.200*	*0.182*	*8.873*	*3.531*
CI_S_1	33	62	247	FZCN_AUT	0.132	−10.745	0.677	−0.241	22.442
					0.019	*2.907*	*0.107*	*7.619*	*2.628*
CI_S_2	22	53	220	FZCN_AUT	0.108	−12.937	0.573	−0.301	21.224
					0.019	*2.984*	*0.176*	*7.395*	*2.431*
CI_S+H_0.5	91	91	316	FZCN_MAN, STSL_MAN			0.810	0.958	27.167
							0.077	*0.013*	*4.216*
CI_S+H_1	79	89	300	FZCN_MAN, STSL_MAN			0.839	0.962	23.914
							0.054	*0.009*	*3.349*
CI_S+H_2	60	78	266	FZCN_MAN, STSL_MAN			0.843	0.962	19.424
							0.047	*0.010*	*2.713*
CI_S+H_0.5	93	92	316	FZCN_AUT, STSL_AUT			0.666	0.905	38.563
							0.087	*0.019*	*4.147*
CI_S+H_1	78	89	300	FZCN_AUT, STSL_AUT			0.730	0.920	33.259
							0.061	*0.018*	*3.508*
CI_S+H_2	62	79	266	FZCN_AUT, STSL_AUT			0.691	0.905	30.945
							0.072	*0.026*	*3.342*

For the independent variables the prefix refers to the information extracted: STSL — standardized total length of hardwood stems; FZCN — fuzzy pixel count for shrub class. Postfixes MAN and AUT refer to manual and automated image extraction, respectively. For the dependent variable CI: H = hardwood, S = shrub for each height threshold (m) given as the final character. Values in italics are the standard deviations from the 1000 resampling iterations.

which the automated method detected shrub competition presence while the manual method did not (i.e. the large range of x values for $y=0$). This was due to confusion between shrub and dark soil in the classification.

3.2.2. Competition index (CI) modeling

Table 2 shows the manual and automated modeling results for the shrub, hardwood, and combined shrub-hardwood competition indices. The model fit statistics are mean values for the 1000 iterations that were implemented using varied random samples. The standard deviations of these statistics are also given in italics. Manual extraction produced the best model fit for all competition response variables with EF>0.70 for all models. Goodness of fit statistics improved when competition height thresholds were used, showing that the competition signal in the imagery was stronger for larger trees, as expected. Hardwood competition was slightly better predicted than shrub competition, having a higher EF for the 0.5 and 2 m height thresholds.

Automated extraction produced lower goodness of fit statistics and higher standard deviations for estimated parameters. Automated model EFs ranged from 0.57 for shrub competition above 2 m in height to 0.70 for shrub-hardwood competition above 1 m. Hardwood competition was better modeled than shrub competition and model fits improved with increasing height threshold. However, for shrubs and hardwood +shrub, at the 2 m threshold, reduced model fits were observed, as this height threshold was close to the mean height of shrub competition in the plots, considerably increasing the number of zero cases for the dependent (i.e. field) variable. This caused greater variability where observed values were zero and predicted values were greater than 0 increasing the overall model bias. This effect was not observed for the hardwood competition modeling because hardwoods were typically taller than the 2 m height threshold. The coefficients from the hardwood+shrub model are not included in the table because they are the same as that given for the bivariate models.

Scatterplots for the competition index models with height threshold of 0.5 m are shown in Fig. 7. They reinforce the results given in Table 2, showing much lower residual spread around the modeled lines for the manual results than automated results. Both manual and automated results fit the 1:1 line well, but errors for the automated method are larger towards the upper end of the observed data range for both shrub and hardwood competition.

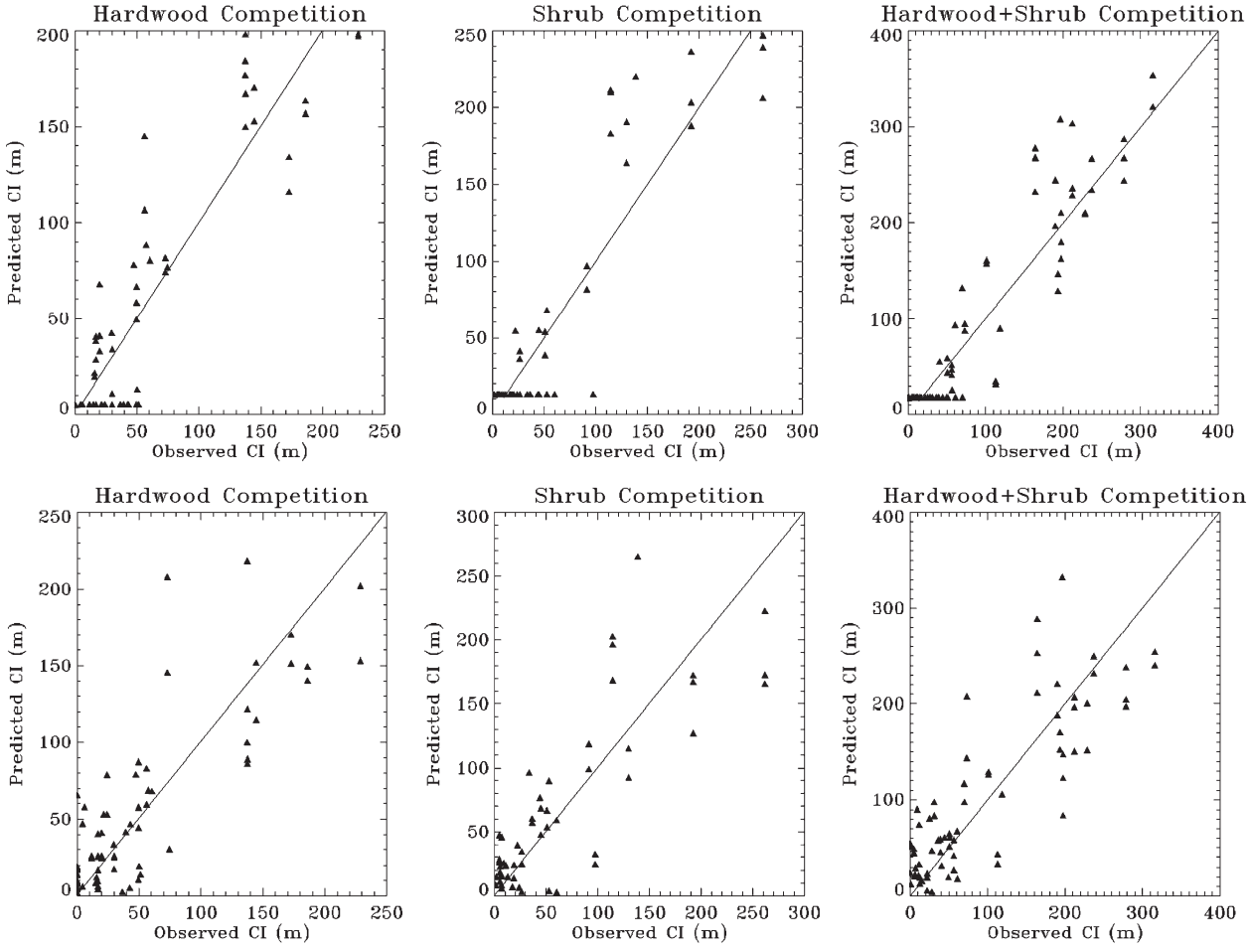

Fig. 7. Scatterplots of hardwood and shrub competition indices predicted from imagery using manual (top) and automated (bottom) methods versus the field measured (observed) competition index for competition >0.5 m in height. The solid 1:1 lines depict the relation $y=\hat{y}$.

3.2.3. Competition stem density modeling

Table 3 shows the modeling results for competition stem density. Again, the manual results outperform the automated extraction, but similar trends were seen. The height thresholds had a strong effect on model quality. For hardwood competition, larger height thresholds improved model prediction accuracy. For shrub competition, the best model was obtained with the 1 m threshold. At the 2 m threshold, model bias increased slightly, reducing the EF statistic. However, MAE decreased consistently with increasing height thresholds again due to the reduction in the number of non-zero cases.

Fig. 8 shows scatterplots for the stem density competition models at the 2 m height threshold. The 2 m threshold is shown because it produced the best overall result for stem density. The manual line fits appear suitable, without strong biases. However, as with the competition index, larger errors are seen for larger observed values in the automated results.

4. Discussion

This research was largely exploratory and intended to determine if there was potential for automated competition assessment using very high resolution leaf-off imagery. As the first known attempt at this, and to serve as a baseline for further research, the methods used were adapted from common image processing methods. The results showed that for the site conditions and image data of this study, strong relations exist between image and field measures of competition. The automated estimates compared favorably with the manual estimates but had larger error, particularly where no competition was present, or in the upper range of competition abundance. Although generalization to other boreal conditions cannot be made from this initial study, the methods indicate good potential for further development in treatment decision making. For example, from the results of this study, manual competition assessment would produce a mean error for estimates of stem

Table 3
Model results for competition stem density (stems/hectare)

Dependent variable	Mean	Stdv	Max	Independent variable(s)	Model parameters		Model fit statistics		
					Slope	Offset	EF	BIAS	MAE
SD_H_0.5	5378	6497	29,360	STSL_MAN	257.5	687.9	0.460	12.82	3182.66
					27.9	*330.4*	*0.227*	*1053.82*	*434.54*
SD_H_1	4970	6063	26,530	STSL_MAN	239.1	608.0	0.574	−0.59	2668.05
					23.9	*283.3*	*0.169*	*874.97*	*363.43*
SD_H_2	3578	4982	19,455	STSL_MAN	186.7	163.4	0.816	−16.40	1316.55
					14.6	*145.2*	*0.056*	*465.54*	*194.89*
SD_H_0.5	5478	6593	29,360	STSL_AUT	263.5	−107.5	0.453	30.96	2917.46
					31.8	*317.5*	*0.238*	*1076.67*	*453.35*
SD_H_1	5078	6148	26,530	STSL_AUT	245.0	−130.7	0.533	27.22	2553.28
					27.5	*281.8*	*0.202*	*915.63*	*383.41*
SD_H_2	3686	5048	19,455	STSL_AUT	191.4	−409.8	0.662	20.08	1805.24
					20.0	*182.9*	*0.132*	*638.32*	*236.10*
SD_S_0.5	11,709	12,551	47,046	FZCN_MAN	304.8	4177.6	−0.040	445.70	7893.13
					48.3	*795.5*	*0.471*	*3210.77*	*1658.58*
SD_S_1	5225	8725	32,897	FZCN_MAN	175.6	741.5	0.834	21.65	2185.97
					14.6	*250.9*	*0.075*	*829.34*	*365.27*
SD_S_2	2772	6568	26,884	FZCN_MAN	120.6	−349.3	0.812	−55.69	1466.41
					14.9	*160.0*	*0.089*	*614.15*	*242.56*
SD_S_0.5	12,032	12,680	47,046	FZCN_AUT	339.4	945.0	0.057	99.75	7480.56
					52.9	*691.6*	*0.399*	*2939.66*	*1451.76*
SD_S_1	5399	8849	32,897	FZCN_AUT	196.9	−1102.1	0.729	−55.30	3108.73
					22.0	*369.2*	*0.088*	*986.10*	*353.98*
SD_S_2	2881	6675	26,884	FZCN_AUT	135.7	−1613.5	0.615	−78.00	2597.29
					21.3	*346.0*	*0.160*	*867.77*	*292.16*
SD_H+S_0.5	17,109	13,743	49,522	FZCN_MAN, STSL_MAN			0.042	0.82	8444.24
							0.477	*0.04*	*1744.75*
SD_H+S_1	10,204	10,768	34,312	FZCN_MAN, STSL_MAN			0.767	0.95	3539.48
							0.081	*0.01*	*547.06*
SD_H+S_2	6349	8272	28,299	FZCN_MAN, STSL_MAN			0.802	0.95	2303.82
							0.060	*0.01*	*333.39*
SD_H+S_0.5	17,533	13,836	49,522	FZCN_AUT, STSL_AUT			0.100	0.78	8381.16
							0.358	*0.05*	*1524.73*
SD_H+S_1	10,486	10,870	34,312	FZCN_AUT, STSL_AUT			0.724	0.92	4152.32
							0.069	*0.02*	*418.47*
SD_H+S_2	6567	8360	28,299	FZCN_AUT, STSL_AUT			0.672	0.90	3464.00
							0.069	*0.02*	*324.59*

For the independent variables the prefix refers to the information extracted: STSL — standardized total line length of hardwood stems; FZCN — fuzzy pixel count for shrub class. Postfixes MAN and AUT refer to manual and automated image extraction, respectively. For the dependent variable stem density (SD): H = hardwood, S = shrub, for each height threshold (m) given as the final character. Values in italics are the standard deviations from the 1000 resampling iterations.

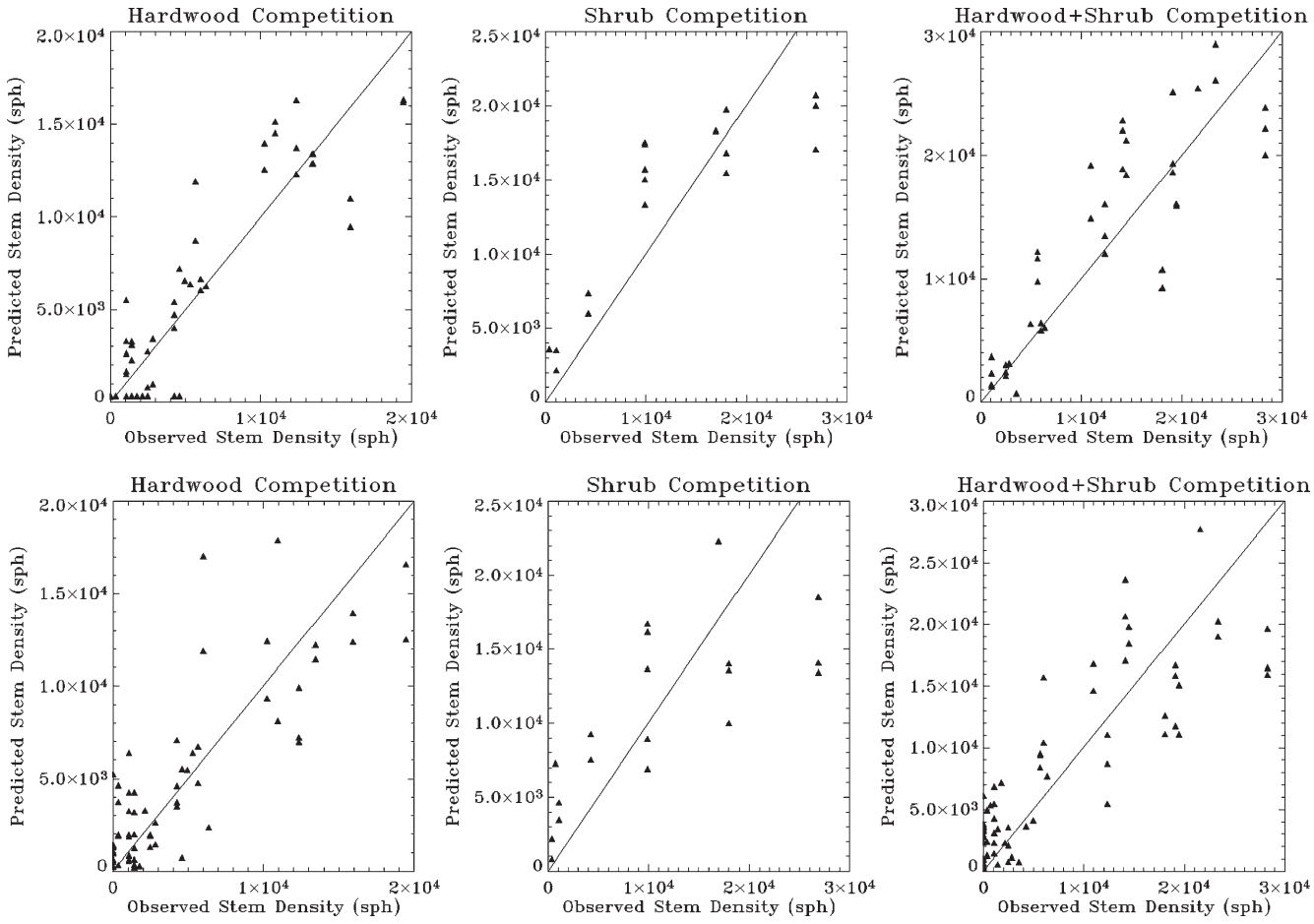

Fig. 8. Scatterplots of hardwood and shrub competition stem density (stems per hectare, sph) predicted from imagery using manual (top) and automated (bottom) methods versus field measured (observed) competition stem density for competition >1 m in height. The solid 1 : 1 lines depict the relation $y=\hat{y}$.

density above 2 m of about 1300 sph for hardwoods, 1500 sph for shrubs, and 2300 sph for shrubs and hardwoods combined. If an approximate threshold for the decision to apply a competition control treatment is 5000 sph of hardwood and shrub competition (Fox, 2004 *pers. comm.*), it appears that the results of the manual extraction could be used to identify areas meeting this criteria. For the automated results, errors in competition stem density would be ~1.5 times larger, reducing the precision of such a treatment threshold estimate. A potential solution to combine the positive attributes of each type of analysis would be to use automated analysis to process the bulk of the data, with manual interpretation or field based surveys used to evaluate areas identified from the automated results to be within ±2300 sph of the desired competition threshold.

The above statements assume that both the automated and manual results in this study could be replicated in similar forest conditions. To better evaluate the potential advantage of manual interpretation over automated analysis, results of several independent interpreters should be used in an analysis of precision and accuracy. This should be combined with a relative cost analysis for evaluation of operational potential. Possible improvements to the manual extraction method are limited, but delineation of hardwood stems and interpretation of shrub areas would improve if conducted in a stereo workstation environment. This however, would require additional image acquisition, storage and processing time that would add to an already laborious task. Automated extraction provides the capability for rapid image processing, but improvements are required for it to be comparable to manual extraction. For automated processing, classification was the most important component affecting accuracy, as it was used as a direct measure of shrub competition and to constrain candidate lines for hardwood competition. Other automated methods may be able to aid in extracting the required information and need to be explored. For example, there are numerous other approaches to texture characterization that could improve results, especially methods that evaluate texture over multiple scales based on fractal analysis (Emerson et al., 1999), wavelets (Zhu & Yang, 1998), or co-occurrence texture (Coburn & Roberts, 2004). The use of other classification methods that incorporate spatial properties, such as contextual classification (Gong & Howarth, 1992), neural networks, or object-oriented classification should also be investigated.

The measure of competition to be modeled is an important operational consideration. The competition index was more strongly related to image measurements than stem density and would improve the ability to determine whether a given competition threshold has been met. However, the competition

index values do not have direct meaning and would require calibration to be used in decision-making. A problem with both measures of competition is that plots with a large number of small competitors could have similar values to plots with a small number of large stems. The influence of these two conditions on crop tree growth is different and important to identify. The use of a height threshold as presented in this study helps to reduce such error and was warranted for the given vegetation age and structure in the sites. Other competition indices could also be evaluated that may improve the models.

The problem of woody debris being oriented in a similar direction to that of the relief displaced woody stems presents a major difficulty for the automated methods. One approach to help reduce this source of error is to include stem width and use a threshold to distinguish competition from woody debris. However, in this dataset, woody debris were in some cases of similar width to the competition. As a simple practical solution, for image plots identified with high competition, a visual scan could be conducted to assess whether woody debris were a substantial source of error.

The long-term objective of this research is to develop an efficient and robust remote sensing methodology for monitoring forest regeneration under basic and extensive silviculture management. The high resolution sampling approach described here was intended to provide detailed and accurate information on competition from leaf-off imagery. Combining this with automated methods for coniferous crop tree detection, delineation and measurement (Pouliot & King, 2005; Pouliot et al., 2002, 2005) would provide capability for integrated regeneration assessment. The results could then be aggregated to strata level estimates following the procedure currently used for plot based field sampling for regeneration assessments. Further research will evaluate potential improvements to the methods developed here as well as other sensors such as lidar or radar that may help to identify differences between ground covers and competition. Most important is evaluation with a dataset of greater coverage to more fully identify conditions where the methods succeed or fail and the frequency with which such conditions can be expected to occur in a more operational setting.

5. Conclusion

Using a combination of spectral, textural and linear object information automatically extracted from leaf-off very high-resolution imagery, strong models were produced for shrub, hardwood, and combined shrub + hardwood regeneration competition estimation. As this is the first study of its kind, common automated methods were selected to serve as a baseline for further research. Further refinement of the methodology should improve model quality. The study also included competition estimates derived from a single manual interpretation that were slightly more accurate than the automated estimates. It is proposed that automated methods be used in a first pass to provide maps of areas of high and low competition (requiring obvious treatment or no need for treatment), followed by manual interpretation of the more uncertain areas to determine if some of them also need treatment. Further research to determine operational potential should emphasize this combined methodology and include testing of several interpreters and a larger dataset. The ability to evaluate competition abundance from high-resolution imagery coupled with automated conifer tree detection and delineation analysis greatly increases regeneration assessment capabilities and renders the costs associated with a remote sensing approach more favorable.

Acknowledgements

This research was funded by grants to D. King and scholarships to D. Pouliot from the Natural Sciences and Engineering Research Council of Canada. The authors would like to thank Mark Lindsay, Wayne Bell, Duncantech Ltd. (now Redlake Inc.), Wiskair Ltd., and Buchanan Forest Products Ltd. for their contributions to this research.

References

Bell, F. W., (2001). *Forest Vegetation Management Specialist, Ontario Forest Research Institute*. Ontario Ministry of Natural Resources. Personal communication.

Bell, F. W., Ter-Mikaelian, M. T., & Wagner, R. G. (2000). Relative competitiveness of nine early successional boreal forest species associated with planted jack pine and black spruce seedlings. *Canadian Journal of Forest Research*, *30*, 790–800.

Brown, R., & Fletcher, V. (1999). Application of CASI remote sensing to classification of backlog not satisfactorily restocked forest in northern British Columbia. *Proceedings of the International Forum on Automated Interpretation of High Spatial Resolution Digital Imagery for Forestry.* 10–12 February 1998, Victoria, B.C. Pacific Forestry Centre, Canadian Forest Service, Natural Resources Canada, Victoria, B.C. pages 155–160.

Burton, P. J. (1993). Some limitations inherent to static indices of plant competition. *Canadian Journal of Forest Research*, *23*, 2141–2151.

Coburn, C. A., & Roberts, A. C. B. (2004). A multiscale texture analysis procedure for improved forest stand classification. *International Journal of Remote Sensing*, *25*, 4287–4308.

Comeau, P. G., Braumandl, T. F., & Xie, C. (1993). Effects of overtopping vegetation on light availability and growth of Engelmann spruce (*Picea engelmannii*) seedlings. *Canadian Journal of Forest Research*, *23*, 2044–2048.

Draper, N., & Smith, H. (1998). *Applied regression analysis* (3rd edition). John-Wiley and Sons Inc., 736 pp.

Emerson, C. W., Lam, N. S., & Quattrochi, D. (1999). Multi-scale fractal analysis of image texture and pattern. *Photogrammetric Engineering and Remote Sensing*, *65*, 51–61.

Fox, B. (2004). *Forest Health and Silviculture Specialist*. Ontario Ministry of Natural Resources. Personal communication.

Franklin, S. E., Hall, R. J., Moskal, L. M., Maudie, A. J., & Lavigne, M. B. (2000). Incorporating texture into classification of forest species composition from airborne multispectral images. *International Journal of Remote Sensing*, *21*, 61–79.

Goba, N., Pala, S., & Narraway, J. (1982). *An instruction manual on the assessment of regeneration success by aerial survey.*Toronto, Ont.: Ontario Ministry of Natural Resources publication, 57 pp.

Gong, P., & Howarth, P. J. (1992). Frequency-based contextual classification and gray-level vector reduction for land-use identification. *Photogrammetric Engineering and Remote Sensing*, *58*, 423–437.

Gougeon, F. A., & Leckie. D. G. (1999). Forest regeneration: individual tree crown detection techniques for density and stocking assessments. *Proceedings of the International Forum on Automated Interpretation of High Spatial Resolution Digital Imagery for Forestry.* 10–12 February 1998, Victoria,

B.C. Pacific Forestry Centre, Canadian Forest Service, Natural Resources Canada, Victoria, B.C. pages 169–177.

Haddow, K. A., King, D. J., Pouliot, D. A., Pitt, D. G., & Bell, F. W. (2000). Early regeneration conifer identification and competition cover assessment using airborne digital camera imagery. *Forestry Chronicle*, *76*, 915–928.

Hall. R.J., (1984). *Use of large-scale aerial photographs in regeneration assessments. Information Report NOR-x-264*, Northern Forest Research Centre, Canadian Forest Service, 31 pp.

Hall, R. J., & Aldred, A. H. (1992). Forest regeneration appraisal with large-scale aerial photographs. *Forestry Chronicle*, *68*, 142–150.

Hall-Beyer, M. (2004). GLCM texture: a tutorial. http://www.ucalgary.ca/~mhallbey/texture%20tutorial/texture_tutorial.html. Accessed 10/09/2005.

Haralick, R. M., Shanmugam, K., & Dinstein, I. (1973). Textural features for image classification. *IEEE Transactions on Systems, Man, and Cybernetics SMC*, *3*, 610–621.

Lillesand, T. M., & Kiefer, R. W. (2000). *Remote sensing and image interpretation* (4th edition). Toronto: John Wiley and Sons, 715 pp.

Mayer, D. G., & Bulter, D. G. (1993). Statistical validation. *Ecological Modelling*, *68*, 21–32.

Morris, D. M., MacDonald, G. B., & McClain, K. M. (1990). Evaluation of morphological attributes as response variables to perennial competition for 4-year-old black spruce and jack pine seedlings. *Canadian Journal of Forest Research*, *20*, 1696–1703.

Peddle, D. R., & Franklin, S. E. (1991). Image texture processing and data integration for surface pattern discrimination. *Photogrammetric Engineering and Remote Sensing*, *57*, 413–420.

Pellikka, P. K. E., King, D. J., & Leblanc, S. G. (2000). Quantification and removal of bidirectional effects in aerial CIR imagery of deciduous forest using two reference land surface types. *Remote Sensing Reviews, Special Issue on "Multi-angle Measurements and Models"*, *vol. 19* (pp. 259–291).

Pitt, D. G., & Glover, G. R. (1993). Large-scale 35-mm aerial photographs for assessment of vegetation-management research plots in Eastern Canada. *Canadian Journal of Forest Research*, *23*, 2159–2169.

Pitt, D. G., Runesson, U., & Bell, F. W. (2000). Application of large- and medium-scale aerial photographs for forest vegetation management: a case study. *Forestry Chronicle*, *76*, 903–913.

Pouliot, D. A., & King, D. J. (2005). Approaches for optimal automated individual tree crown detection in young regenerating coniferous forests. *Canadian Journal of Remote Sensing*, *31*, 256–267.

Pouliot, D. A., King, D. J., Bell, F. W., & Pitt, D. G. (2002). Automated tree crown detection and delineation in high-resolution digital camera imagery of coniferous forest regeneration. *Remote Sensing of Environment*, *82*, 322–334.

Pouliot, D. A., King, D. J., & Pitt, D. G. (2005). Development and evaluation of an automated tree detection–delineation algorithm for monitoring regeneration coniferous forests. *Canadian Journal of Forest Research*, *35*, 2332–2345.

Price, R., & Davison, D. (1999). Operational techniques for assessing NSR areas using an airborne multispectral imager (CASI). *Proceedings of the International Forum on Automated Interpretation of High Spatial Resolution Digital Imagery for Forestry.* 10–12 February 1998, Victoria, B.C. Pacific Forestry Centre, Canadian Forest Service, Natural Resources Canada, Victoria, B.C. pages 161–168.

Richards, J. A. (1993). *Remote sensing digital image analysis: an introduction* (2nd edition). Springer-Verlag New York Inc., 340 pp.

Steger, C. (1998). An unbiased detector of curvilinear structures. *IEEE Transactions on Pattern Analysis and Machine Intelligence*, *20*, 537–559.

Ter-Mikaelian, M. T., Wagner, R. G., Bell, F. W., & Shropshire, C. (1999). Comparison of photosynthetically active radiation and cover estimation for measuring the effects of interspecific competition on jack pine seedlings. *Canadian Journal of Forest Research*, *29*, 883–889.

Treitz, P. M., & Howarth, P. J. (2000). Integrating spectral, spatial, and terrain variables for forest ecosystem classification. *Photogrammetric Engineering and Remote Sensing*, *66*, 305–317.

Tuominen, S., & Pekkarinen, A. (2005). Performance of different spectral and textural aerial photograph features in multi-source forest inventory. *Remote Sensing of Environment*, *94*, 256–268.

Wagner, R. G, Bell, F. W., & Campbell, R. A. (2001). Vegetation management. In R. G. Wagner, & S. J. Colombo (Eds.), *Regenerating the Canadian forest: Principles and practices for Ontario* (pp. 431–458). Fitzhenry and Whiteside Ltd.

Walstad, J. D., & Kuch, P. J. (1987). *Forest vegetation management for conifer production.*New York: John Wiley and Sons, 523 pp.

Wang, G. G., Siemens, J. A., Keenan, V., & Philippot, D. (2000). Survival and growth of black and white spruce seedlings in relation to stock type, site preparation and plantation type in southeastern Manitoba. *Forestry Chronicle*, *76*, 775–782.

Wulder, M., Franklin, S. E., & Lavigne, M. B. (1996). High resolution optical image texture for improved estimation of forest stand leaf area index. *Canadian Journal of Remote Sensing*, *22*, 441–449.

Zhu, C., & Yang, X. (1998). Study of remote sensing image texture analysis and classification using wavelet. *International Journal of Remote Sensing*, *19*, 3197–3203.